

RECENT DEVELOPMENTS AND RESULTS OF THE 3I ALGORITHM

A. Chedin, N.A. Scott

Laboratoire de Météorologie Dynamique du CNRS
Ecole Polytechnique, 91128 Palaiseau Cedex, France

E. Andersson, J.F. Flobert

ECMWF, Shinfield Park, Reading, RG2 9AX, England

Summary

As a feedback to the extensive series of experiments carried out at ECMWF and aiming at measuring the impact of satellite data, processed by the 3I (Improved Initialization Inversion) scheme developed at LMD, on middle range weather forecasting, modifications to the algorithm are described and applied to several pathological NOAA-9 and NOAA-10 passes. The main improvements concern the temperature variance/covariance matrix involved in the solution estimation method, the cloud-clearing technique and the introduction of a rain detection test. Significant improvements are obtained and illustrated through comparisons with analyses. They involve layer mean temperatures and an overall tropospheric stability index.

1. INTRODUCTION

At ECMWF, an extensive series of experiments has been carried out using satellite sounding data from the NOAA satellites and the 3I (Improved Initialization Inversion) retrieval scheme developed by the ARA (Atmospheric Radiation Analysis) group at LMD. This algorithm has been run in an experimental suite to produce global data sets. More than 40,000 soundings on average have been produced for each 6 hour period from 30 January 00 UT to 14 February 12 UT, 1987. The quality of these soundings was examined and compared to the quality of operational NESDIS soundings with encouraging results : slightly better quality of 3I products on the average in particular for the lowest layer (1000/850 hPa) ; very little random noise ; slightly better vertical gradients, etc...

(see Flobert et al., 1989). However, problems affecting both algorithms or 3I specifically were identified that led us to either refine some of the solutions adopted in 3I or to add a few new and potentially important tests. These improvements and modifications are described in the next three sections. Section 5 presents a quantitative assessment of these changes applied to several passes (NOAA-9 and NOAA-10 ; 1st February 1987) selected according to the problems they have presented.

2. ESTIMATING THE SOLUTION FROM THE INITIAL GUESS : ROLE OF THE TEMPERATURE VARIANCE / COVARIANCE MATRIX

In the 3I approach, the basis for the retrieval of the "exact" solution is a "maximum a posteriori" probability estimator (see Chedin et al., 1985). It may be written as :

$$b_{\text{MAP}} - \beta_o = S_{\beta} X' \left[X S_{\beta} X' + S_e \right]^{-1} \begin{pmatrix} y_e - y_o \end{pmatrix} \quad (1)$$

where b_{MAP} is the estimator of β , β_o , y_o , the initial guess, for respectively, temperature and associated brightness temperatures, y_e the observed brightness temperatures, X the kernel including transmittances, S_e and S_{β} the covariance matrices of the error vector e ($y = X\beta + e$) and β .

Since it starts from an optimum initial guess, which is the situation (or the mean of an ensemble of situations) closest to the observed situation among those archived in the TIGR (TOVS Initial Guess Retrieval) data set, the "3I" method aims at estimating the difference between the parameters and their values for the closest situation rather than the parameters themselves as in Eq. (1). This can be rewritten as :

$$\beta^* - \beta_o^* = S_{\beta}^* X' \left[X S_{\beta}^* X' + S_e \right]^{-1} \begin{pmatrix} y^* - y_o^* \end{pmatrix} \quad (2)$$

where $\beta^* = b_{\text{MAP}} - \beta_{\text{IG}}$, $y^* = y_e - y_{\text{IG}}$; β_{IG} is the initial guess solution associated with y_{IG} and S_{β}^* is the covariance matrix of β^* .

We have verified that β_o^* , mean of β^* , and y_o^* , the mean of y^* , are both equal to 0, which means that the initial guess retrieval procedure is unbiased. Consequently, Eq. (2) is equivalent to :

$$b_{\text{MAP}} - \beta_{\text{IG}} = S_{\beta}^* X' \left[X S_{\beta}^* X' + S_e \right]^{-1} \begin{pmatrix} y_e - y_{\text{IG}} \end{pmatrix} \quad (3)$$

S_{β}^* may be computed from the "TIGR" data set, as explained in Chedin et al. (1985) where it has been shown that S_{β}^* is much more diagonal than S_{β} which renders the latter way of computing b_{MAP} more attractive than the usual one.

The procedure used up to recently to compute (off-line) S_{β}^* may be summarized as follows :

- among a given air mass class of TIGR (at present : polar, middle and tropical) one situation, labelled i , is selected, corresponding to the temperature profile T^i . A simplified proximity recognition is carried out and the closest element in TIGR (and not the mean of an ensemble of closest) is retained, corresponding to the temperature profile T_{IG}^i value where IG stands for Initial Guess.

S_{β}^* is the variance-covariance matrix of the vectors $T^i - T_{IG}^i$:

$$S_{\beta}^*(i,j) = \frac{1}{K} \sum_{k=1}^K \begin{pmatrix} T_k^i - T_{IG,k}^i \\ T_k^j - T_{IG,k}^j \end{pmatrix} \begin{pmatrix} T_k^j - T_{IG,k}^j \\ T_k^i - T_{IG,k}^i \end{pmatrix}$$

As in the 3I algorithm, the proximity search starts from the brightness temperatures associated to T^i and compare them to those associated to the other situations in TIGR. It takes care of the flags clear/cloudy (the proximity recognition is different) and land/sea (the brightness temperatures are different). It did not take care, up to recently, of the viewing angle, restricted to nadir viewing. 12 matrices S_{β}^* were computed following the above method (3 air masses, land/sea, clear/cloudy).

The results presented in Part 5 of this paper include an important improvement of the method used to compute S_{β}^* matrices :

- i) as in 3I, the viewing angle is no longer restricted to nadir but sampled by the 10 values archived in TIGR ;
- ii) the proximity recognition used is strictly identical to the one included in 3I :
 - one single step in case of clear areas and two steps, including cloud clearing, in case of cloudy areas ;
 - T_{IG}^i is now, as in 3I, the mean of the profiles contained in the so-called distance circle (see Chedin & Scott, 1985) obtained by multiplying the distance to the closest element in TIGR by 1.25. For the purpose of computing the covariance matrix, T_{IG}^i was previously the closest element itself.

Computing S_{β}^* following the exact way T_{IG}^i is obtained in the on-line retrieval algorithm, without any simplification has resulted in a significant improvement of the quality of the results.

3. DECONTAMINATION OF CLOUDY INFRARED RADIANCES

In the 3I approach, cloud clearing of infrared radiances is carried out through the so-called " ψ -method". Following this method, a cleared infrared brightness temperature is obtained by adding to the initial guess value of the channel considered, the difference between the observed and the initial guess values of a microwave channel, almost insensitive to clouds and peaking approximately at the same levels :

$$\psi^{HIRS}(i) = T_{closest}^{HIRS}(i) + \left[T_{obs}^{MSU}(j) - T_{closest}^{MSU}(j) \right]$$

where $T_{closest}^{HIRS}(i)$ and $T_{closest}^{MSU}(j)$ are, respectively, the brightness temperatures of HIRS-2 channel i and MSU channel j associated with the first initial guess, and $T_{obs}^{MSU}(j)$ is the observed brightness temperature of MSU channel j . When index i takes the values 4, 5, 6 and 15, index j respectively takes the values 3, 2, 2 and 2. For $i = 3$, the reference MSU value is half the sum of $T^{MSU}(3)$ and $T^{MSU}(4)$.

The ψ -method simply relies upon the difference between two channels peaking at approximately the same level and obtained for a situation (the initial guess) relatively close to that observed. This difference is applied to a microwave observation that is almost completely insensitive to the clouds and provides the equivalent (or pseudo) clear infrared observation. More details are given in Chedin et al. (1985) and Chedin (1988). A good coincidence of the microwave and associated infrared observation is thus required to reach an acceptable level of accuracy. This is certainly the case for MSU channel 2 and both HIRS-2 channels 5 and 15. This is more questionable for HIRS-2 channels 3 and 4 and their microwave equivalent (see Fig. 1). For that reason, previous ψ simple approach was refined in the sense that both infrared channels are now cloud cleared using a regression of the form :

$$\psi_{3 \text{ (or 4)}} = a_1 + \sum_{i=2}^4 a_i T_{obs}^{MSU}(i)$$

Coefficients are obtained from the TIGR data base, for each viewing angle and surface elevation and for the two types of terrain (land/sea).

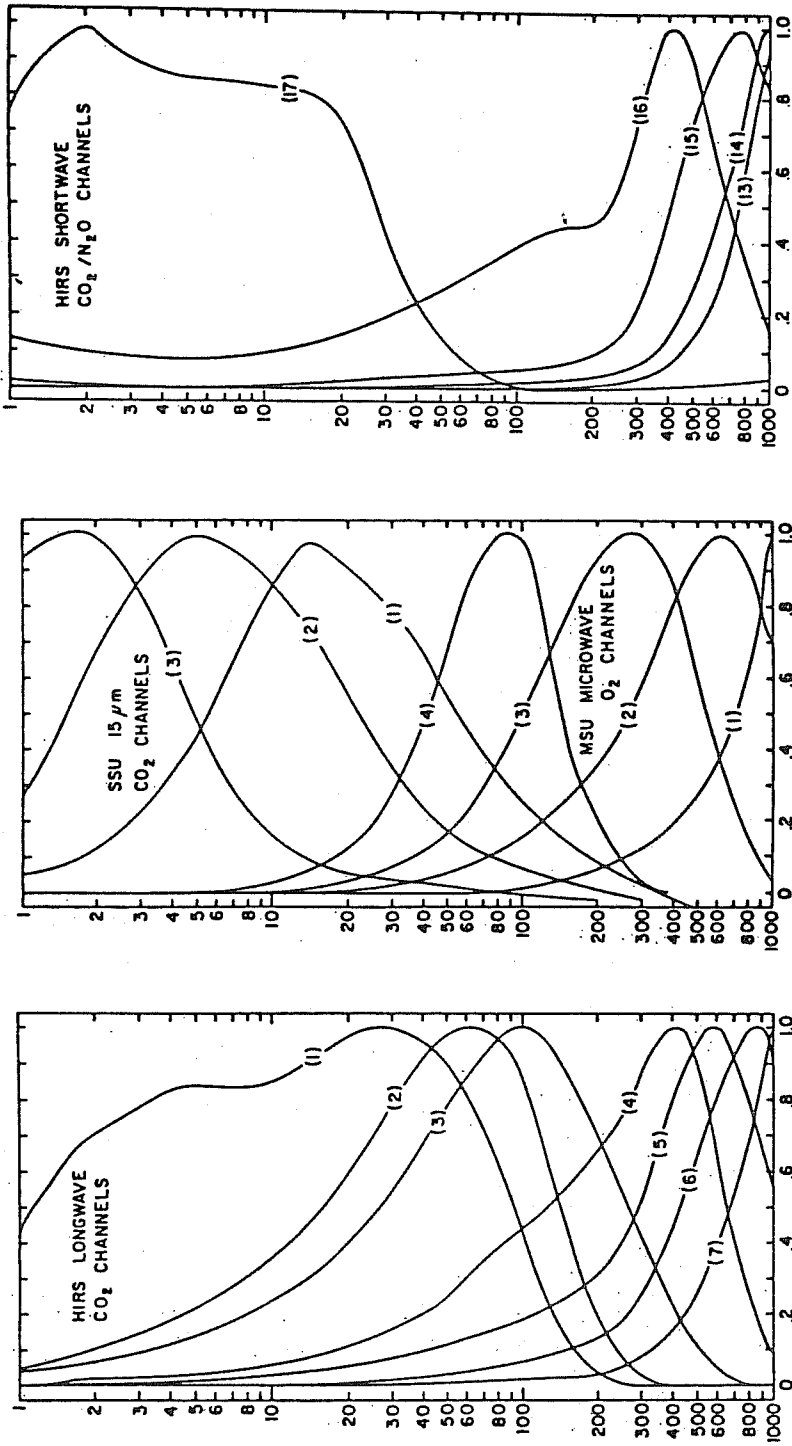


Figure 1 Weighting functions for TOVS channels (from Smith et al., Bull. Amer. Meteor. Soc., 1979).

4. OTHER MINOR BUT POTENTIALLY IMPORTANT CHANGES

These additional modifications have been brought to the 3I algorithm.

i) Low cloud test over sea ice (at day)

A new test has been added to the cloud detection scheme (see Claud et al. 1989) for a better detection of low clouds over sea ice (detected from the microwave surface emissivity) at day. Following that test, an HIRS-2 spot is declared cloudy if the difference between the brightness temperatures of HIRS-2 channels 19 and 8, normalized by the cosine of the solar zenith angle, is larger than 30K. This test results from the difference in albedo of sea ice (lower) and low clouds (higher). This test is restricted to high latitudes.

ii) MSU mapping

A new method has been designed for interpolating MSU observations in the HIRS-2 spots avoiding taking into consideration MSU fields of view too far from the HIRS-2 spot considered.

iii) Assimilation of the SST in the retrieval process

Determination of SST from TOVS may be performed with an acceptable level of accuracy for clear or partly cloudy areas (provided the cloudiness is not too high). This is not the case for overcast areas resulting in additional noise for the retrieved atmospheric (or upper air) parameters. An interesting solution consists in assimilating within the retrieval process itself, the SST values provided by global operational maps available, for example, at the European Center. Such maps originate from AVHRR data processed at NESDIS (Washington) and are regularly updated. This refinement is now introduced, as an option, in 3I.

5. APPLICATION TO A FEW SELECTED (PATHOLOGICAL) PASSES.

COMPARISON TO PREVIOUS RESULTS

Improved in the way described above, the 3I algorithm has been applied to a few passes corresponding to particularly bad comparisons with analyses. They are identified on Fig. 2 and in Table 1.

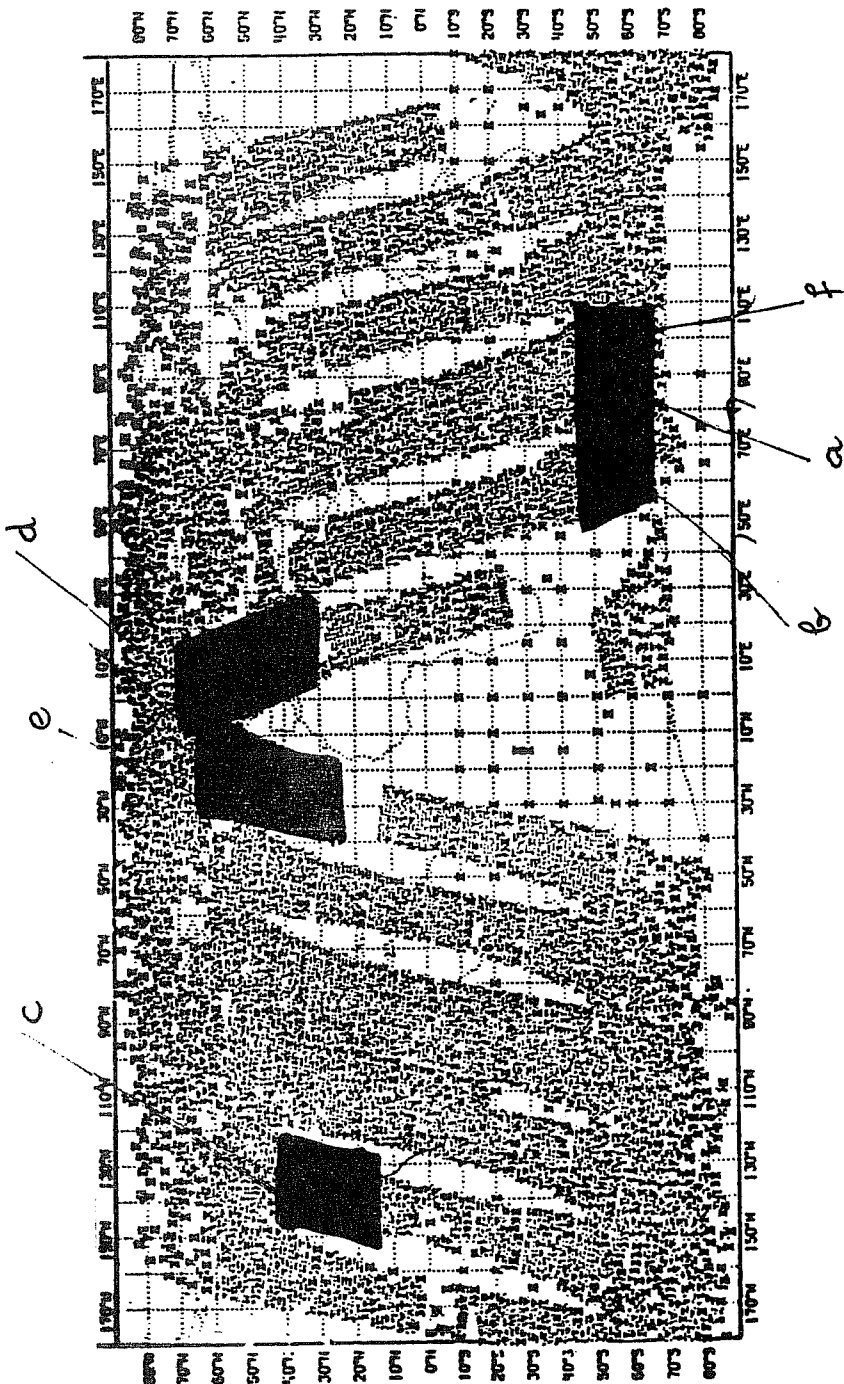


Table 1

| Satellite | Orbit nb. | Time (UT) |
|-----------|-----------|-----------|
| NOAA-9 | 11016 | 9.48 |
| NOAA-9 | 11017 | 11.30 |
| NOAA-9 | 11018 | 12.25 |
| NOAA-9 | 11019 | 13.42 |
| NOAA-10 | 1944 | 9.33 |
| NOAA-10 | 1946 | 13.45 |

Figure 2

Areas selected for the testing of 3I algorithm refinements as described in the preceding sections. February 1st, 1987. a to d : NOAA-9 passes nb. 11016, 11017, 11018 and 11019 respectively ; e and f : NOAA-10 passes 1944 and 1946.

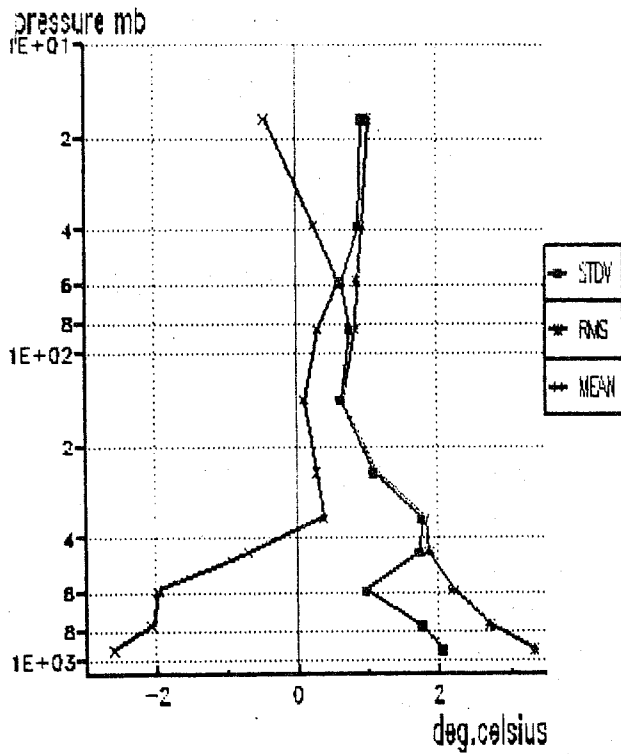


Figure 3a Statistics for the differences between 3I retrieved and ECMWF analysed temperature. Orbit 11016. Before changes.

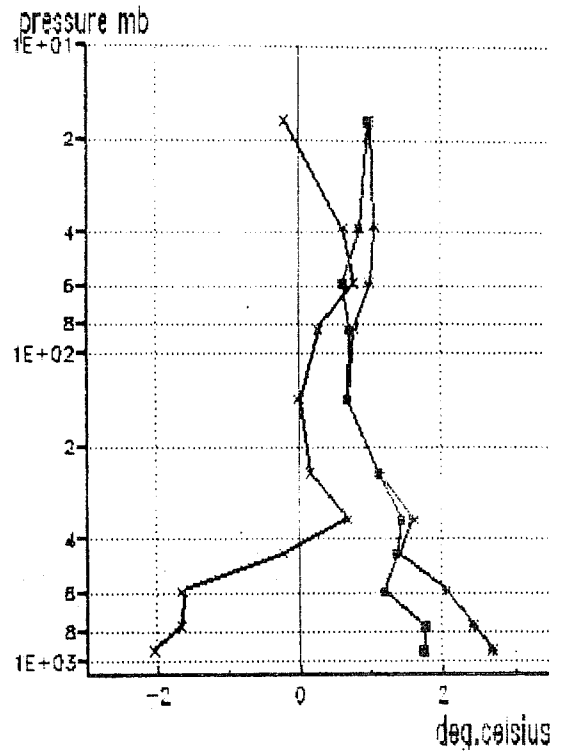


Figure 4a

Same as Fig. 3a. After changes.

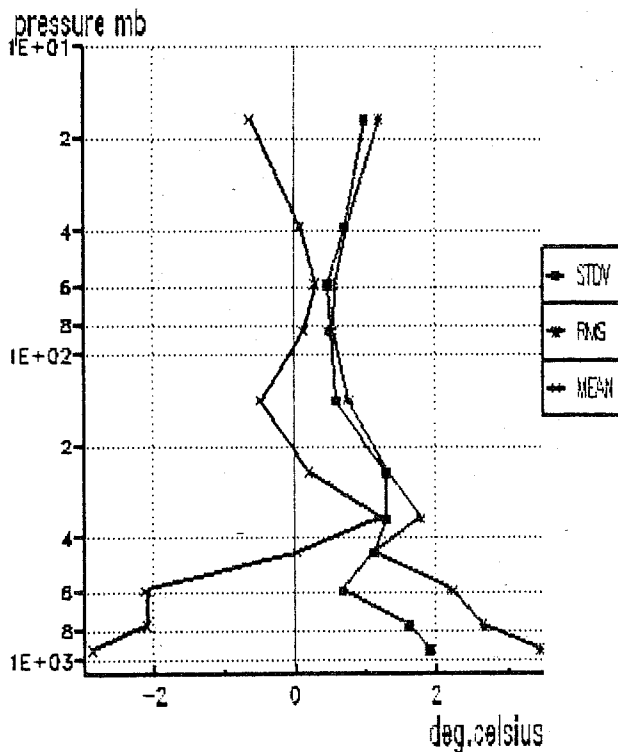


Figure 3b

Same as Fig. 3a. Orbit 11017.

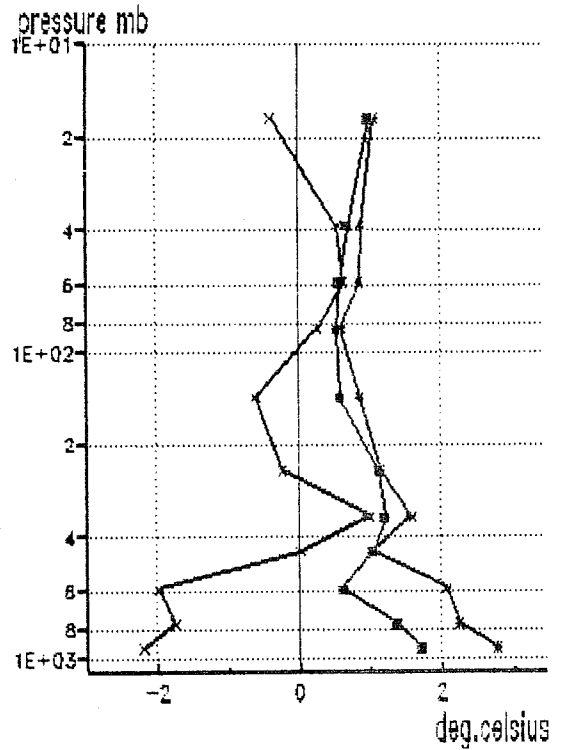


Figure 4b

Same as Fig. 4a. Orbit 11017.

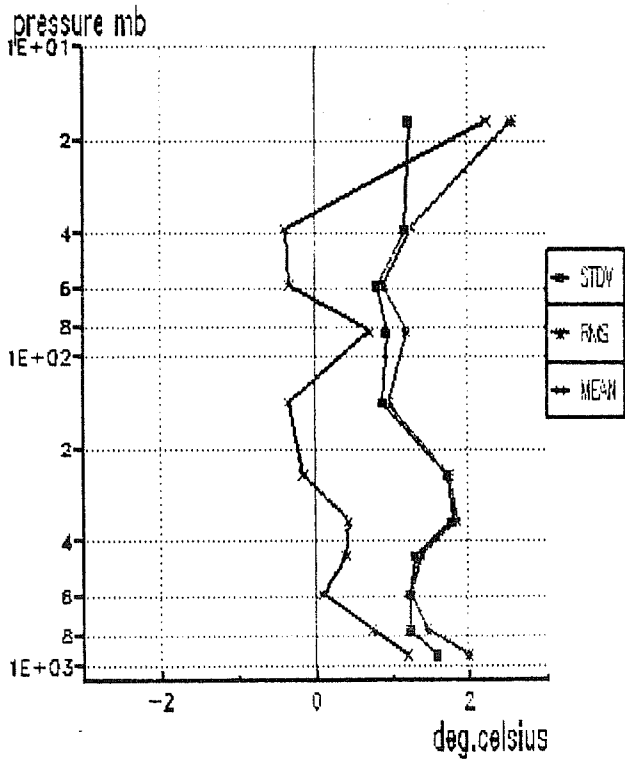


Figure 3c

Same as Fig. 3a. Orbit 11018.

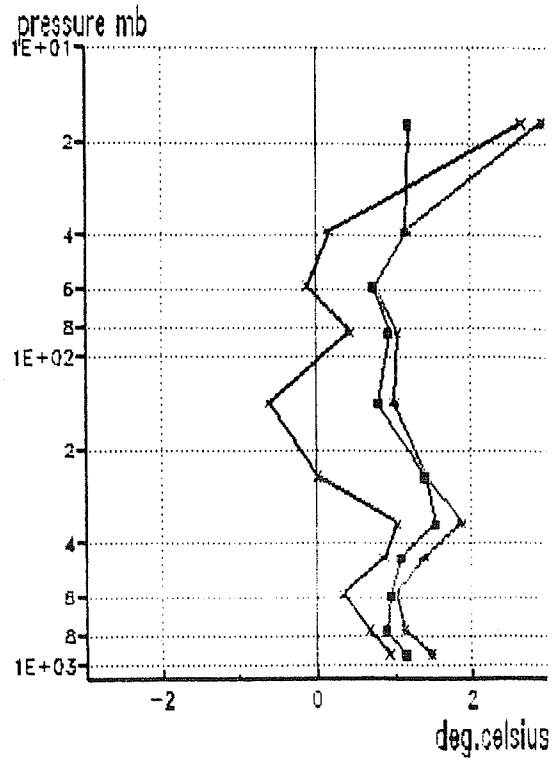


Figure 4c

Same as Fig. 4a. Orbit 11018.

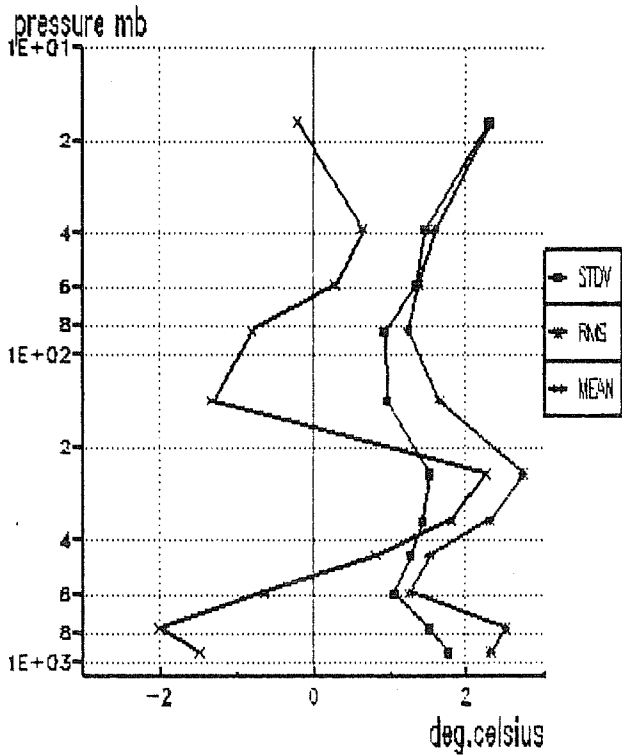


Figure 3d

Same as Fig. 3a. Orbit 11019.

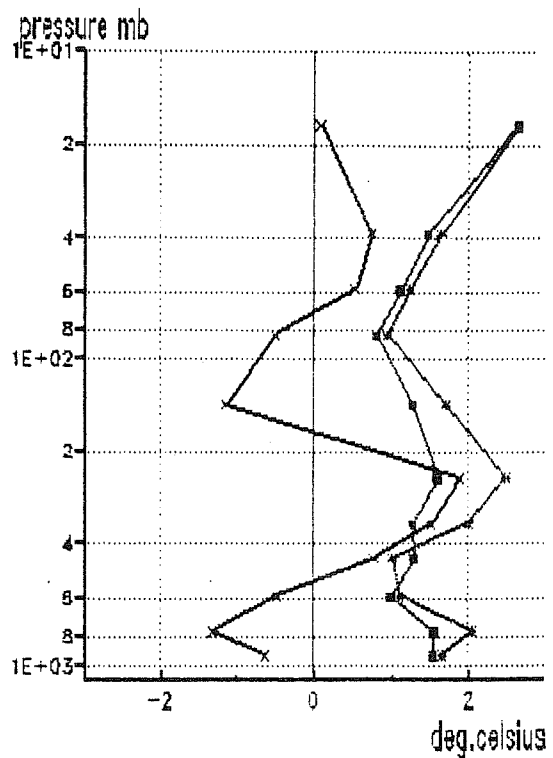


Figure 4d

Same as Fig. 4a. Orbit 11019.

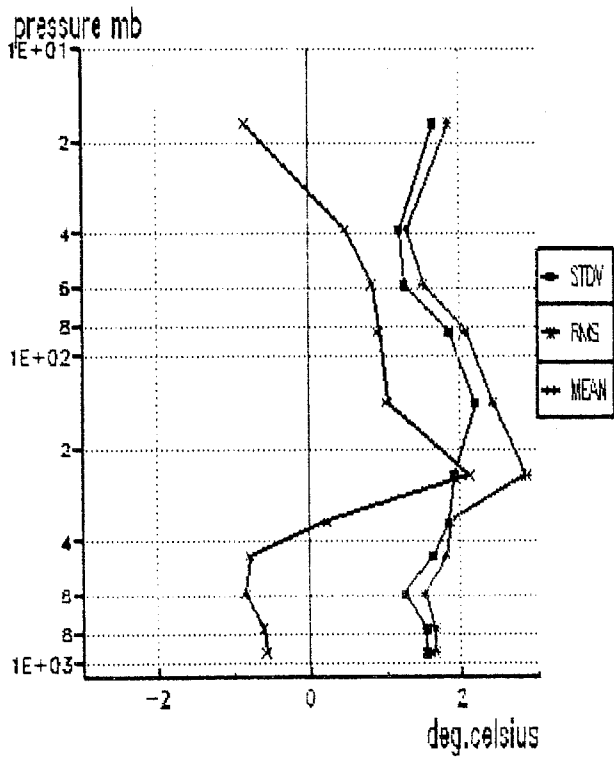


Figure 3e

Same as Fig. 3a. Orbit 1944.

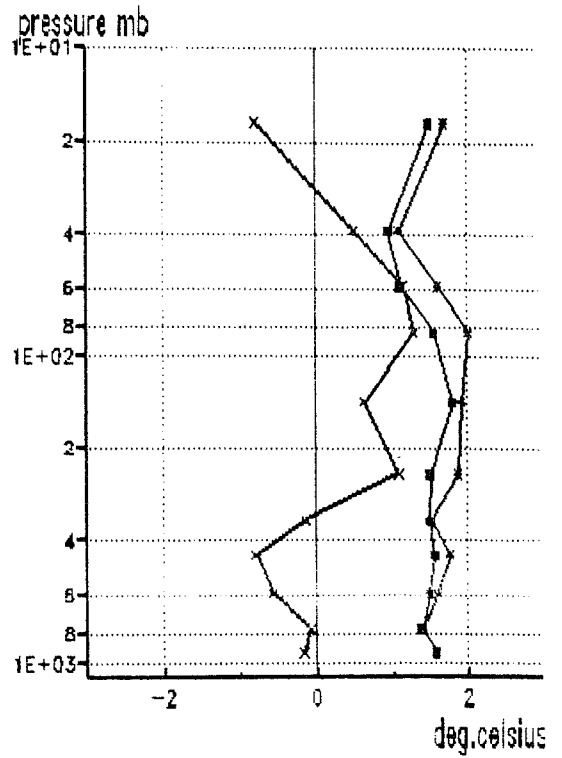


Figure 4e

Same as Fig. 4a. Orbit 1944.

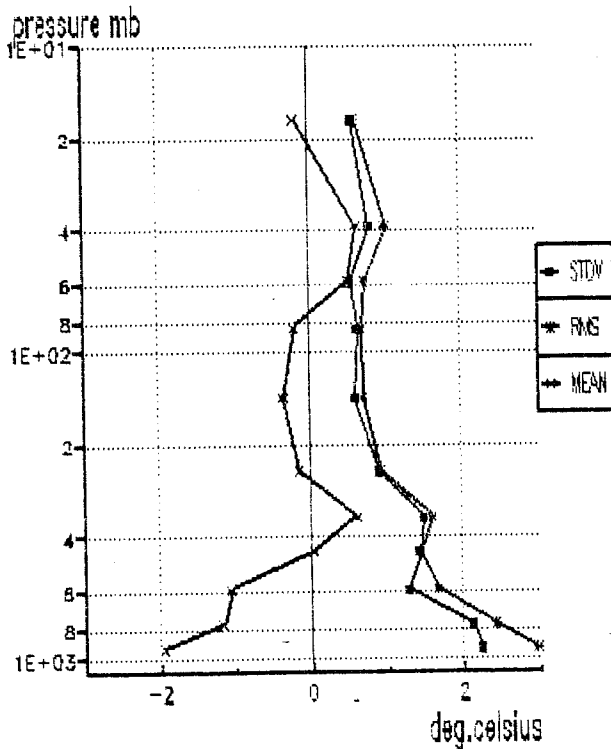


Figure 3f

Same as Fig. 3a. Orbit 1946.

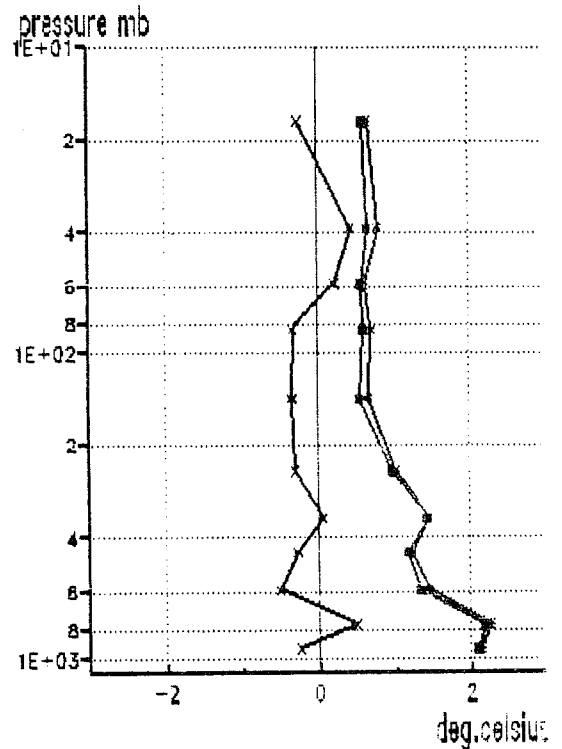


Figure 4f

Same as Fig. 4a. Orbit 1946.

5.1 Impact of the modifications on retrieved temperatures

For all these passes, layer temperature statistics were produced for the differences between 3I before modifications, 3I after modifications and ECMWF corresponding analyses at 12.00 UT. Results are shown on Figs. 3a-3f (before) and on Figs. 4a-4f (after). They bring into evidence the following points :

- there is a general improvement with the modified code over the previous one for both the biases and standard deviations ;
- NOAA-10 passes are spectacularly improved ;
- for three NOAA-9 passes out of four, significant negative biases for the lower troposphere still persist. This is a bit surprising if one considers the proximity of NOAA-9 passes 11017 and 11016 with NOAA-10 pass 1946. Removal of the negative bias is perfect for the latter but not for the former two. It is most likely that the correct explanation lies in an imperfect validation of NOAA-9 synthetic computations.

The next step of the quantitative assessment of the benefit brought by the modifications presented here has consisted in computing and plotting the "stability index" defined by the difference between the temperature (virtual) of the two layers 1000/700 hPa and 500/300 hPa.

5.2 Impact of the modifications on the tropospheric stability index

At ECMWF, a stability index has been defined as : $T(1000-700)-T(500-300)$, where T is the layer mean virtual temperature. The choice of the two above layers gives a measure of overall tropospheric stability (see Andersson et al. 1989). Problems (in particular biases) have been identified over particular areas when comparing values obtained either from 3I or from NESDIS to the first guess model (see Flobert et al., 1989). The impact of the modifications described above has been checked through comparisons of stability index maps derived before and after modifications for all the passes of Table 1. Figs. 5a-5b illustrate an example of such comparisons for one NOAA-9 pass (nb. 11019), actually the most pathological with respect to this parameter. Although original figures are in colour, the improvements between Fig. 5a (before modifications) and 5b (after modifications) is obvious. Darker areas, corresponding to the largest deviations, either negative or positive, have been greatly reduced

and only remain off or over central west Norway and over central Mediterranean. They could be due in part to rain contamination over land.

Although the idea of confronting not only layer retrieved temperatures to corresponding analysed values but also quantities related to temperature gradients in the vertical is very fruitful, it is worth thinking in detail at the definition of such a quantity when satellite products are involved. As presently defined, the stability index raises a problem related to the fact that the lowest layer extends down to 1000 hPa. If the 3I approach has proven being significantly better in the lowest layer, it is also true that the lowest 500 m or 1 km are the most difficult to manage. For that reason, we recommend to define an index better adapted to satellite observation, avoiding the lowest 500 m or 1 km and not obviously sticking to the standard levels. We have undertaken an action in this direction.

5.3 Rain contamination of MSU channels : a study case

As explained in Flobert et al. (1989), several areas of relatively small sizes and characterized by much too cold retrievals in the lower troposphere, turned out to be caused by heavy rain contaminating MSU channels. The simple rain test proposed by Philips (1980) and stating that these channels are likely to be contaminated if the $MSU_2 - MSU_1$ brightness temperature difference is less than twelve degrees was not included in the 3I processing due to a programming oversight. This fact resulted, on February 1st, 1987, on bad "3I forecast" over North America. The origin is due to a front crossing North-East Pacific off Vancouver and observed by NOAA-9 (orbit nb. 11018). For this pass, Fig. 6 illustrates the results of the cloud detection algorithm. Figs. 7a and 7b respectively display the mean cloud amount and mean cloud top pressure as determined by 3I. A zone characterized by an heavy cloudiness and relatively high tops is well identified from the west coast of the USA to the bottom left corner of the figures.

The $MSU_2 - MSU_1$ difference test applied to this orbit is shown on Fig. 8 which clearly brings into evidence a long and relatively narrow band for which difference values are much smaller than 12°C for central areas and up to $16-17^\circ\text{C}$ at the edges. From this case and many others we processed at the same time, we may conclude that a good test limit is 16°C instead of the value recommended by Philips.

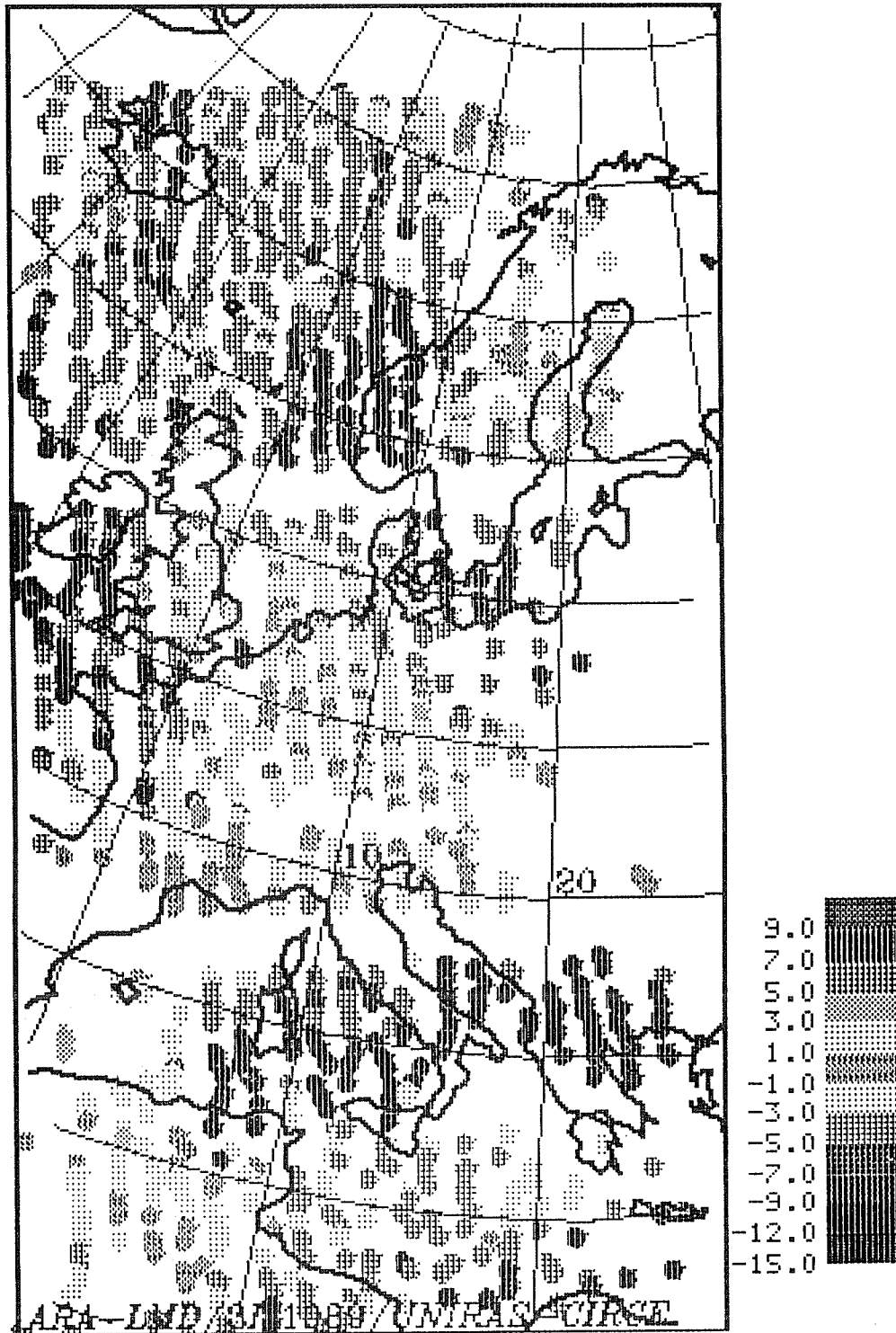


Figure 5a Difference between 3I retrieved and ECMWF first guess for the stability index $[T(1000-700)-T(500-300)]$ before modifications. NOAA-9, pass 11019.

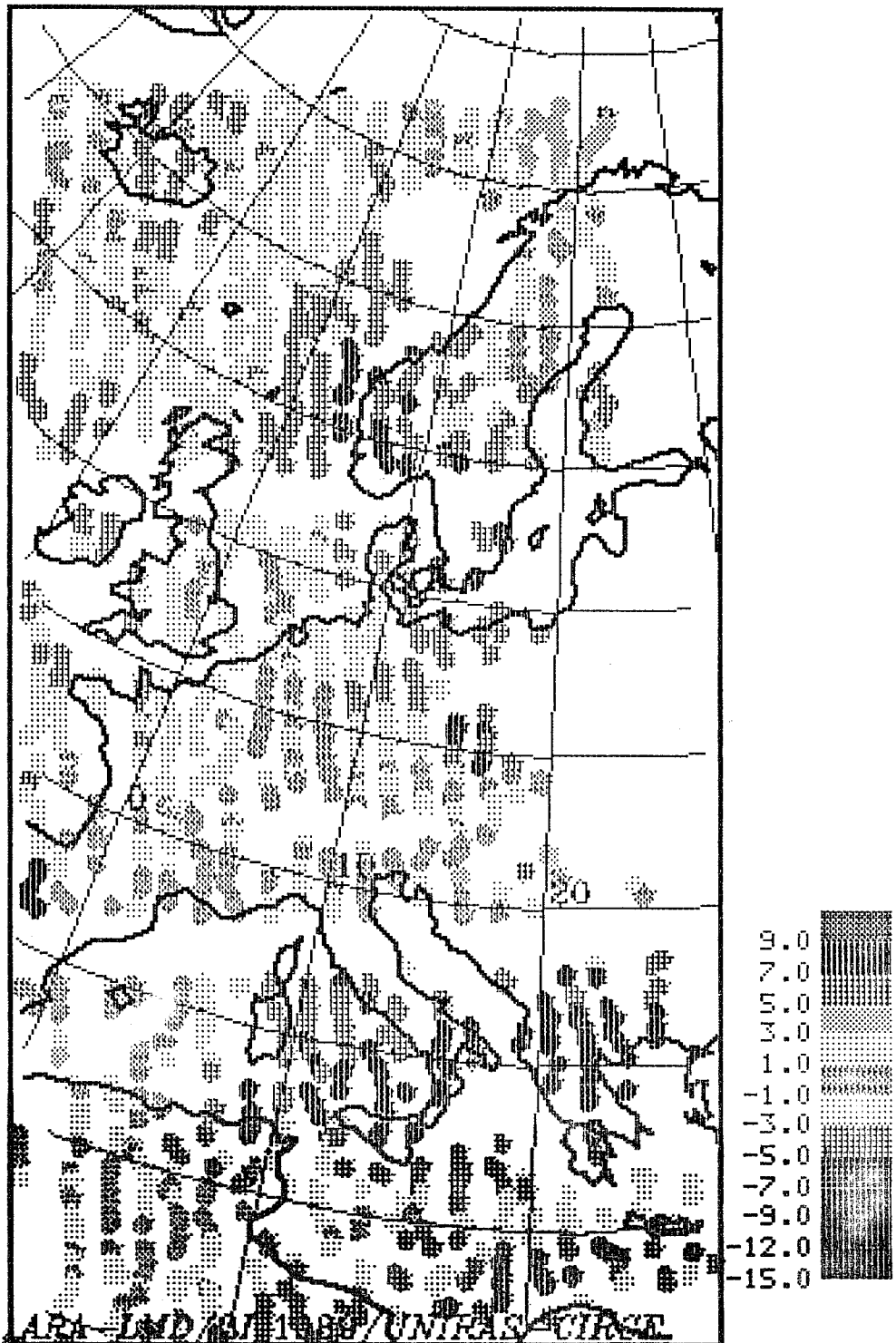


Figure 5b Same as Fig. 5a. After modifications.

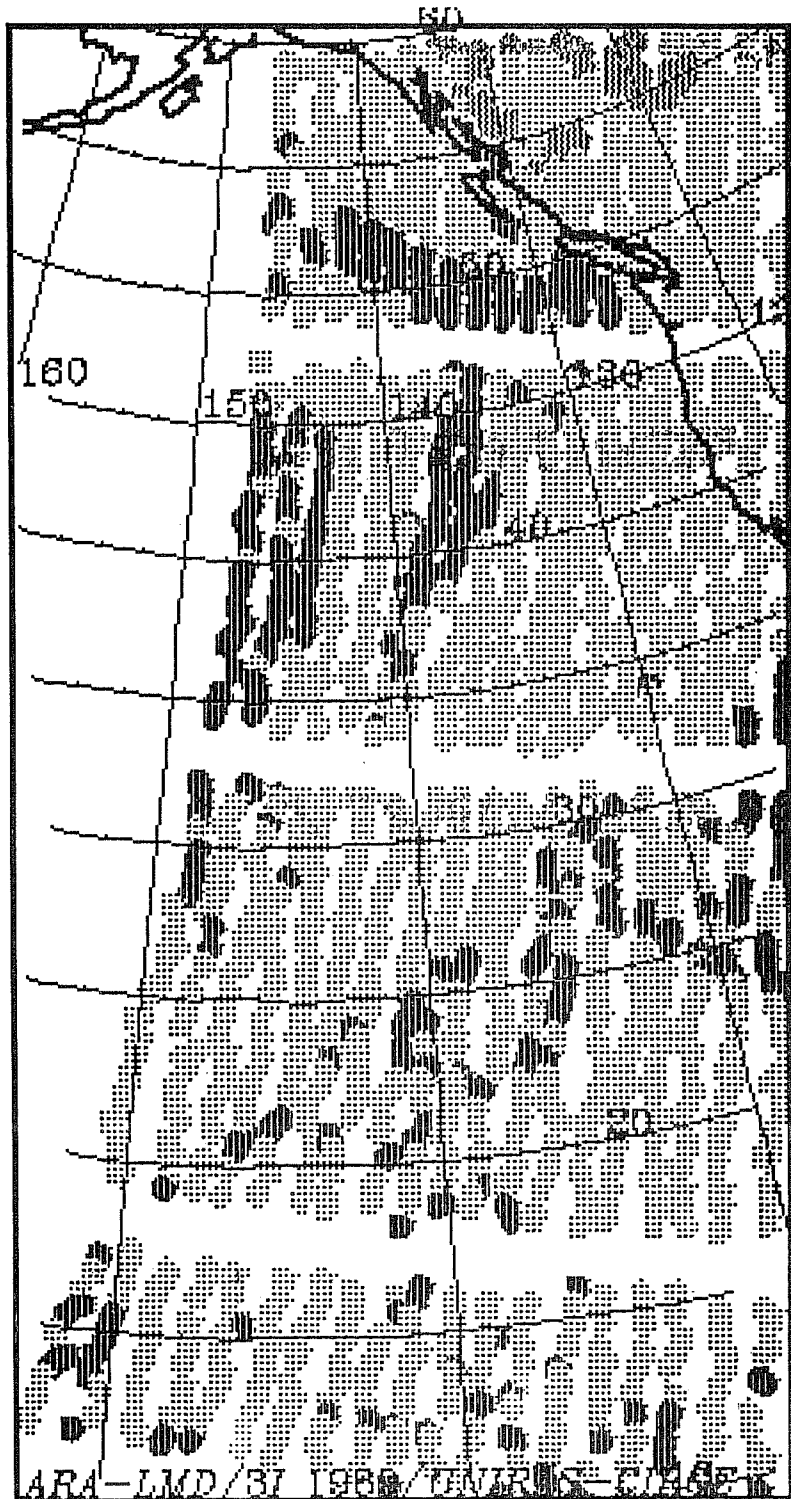


Figure 6 Cloud detection from 3I. Over sea or over land : clouds in grey and clear sky in dark (original in colour). NOAA-9 pass 11019. 1st February 1987.

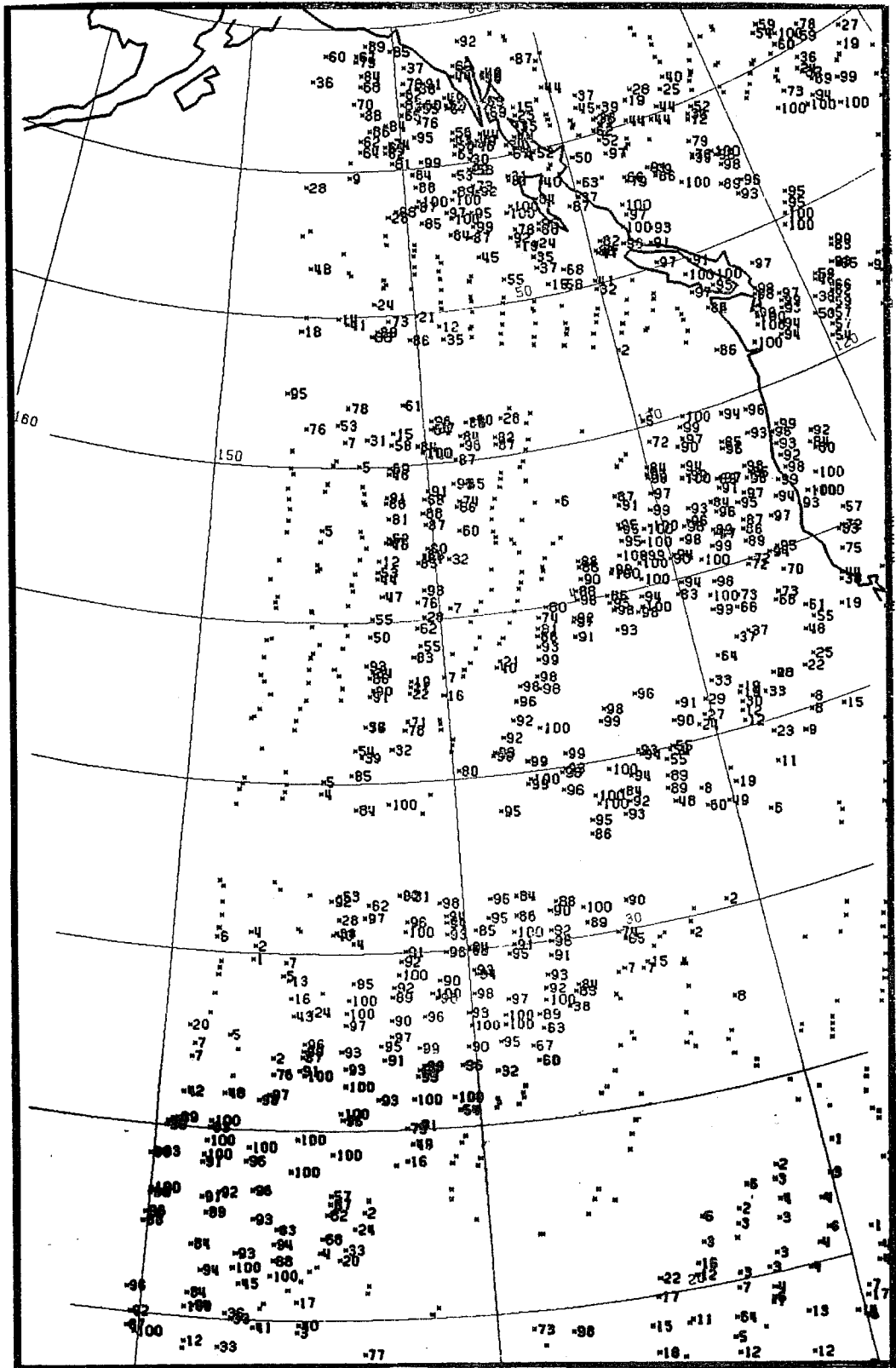


Figure 7a Cloud amounts as determined by 3I for NOAA-9 pass 11018 of 1st February 1987 (in percent).

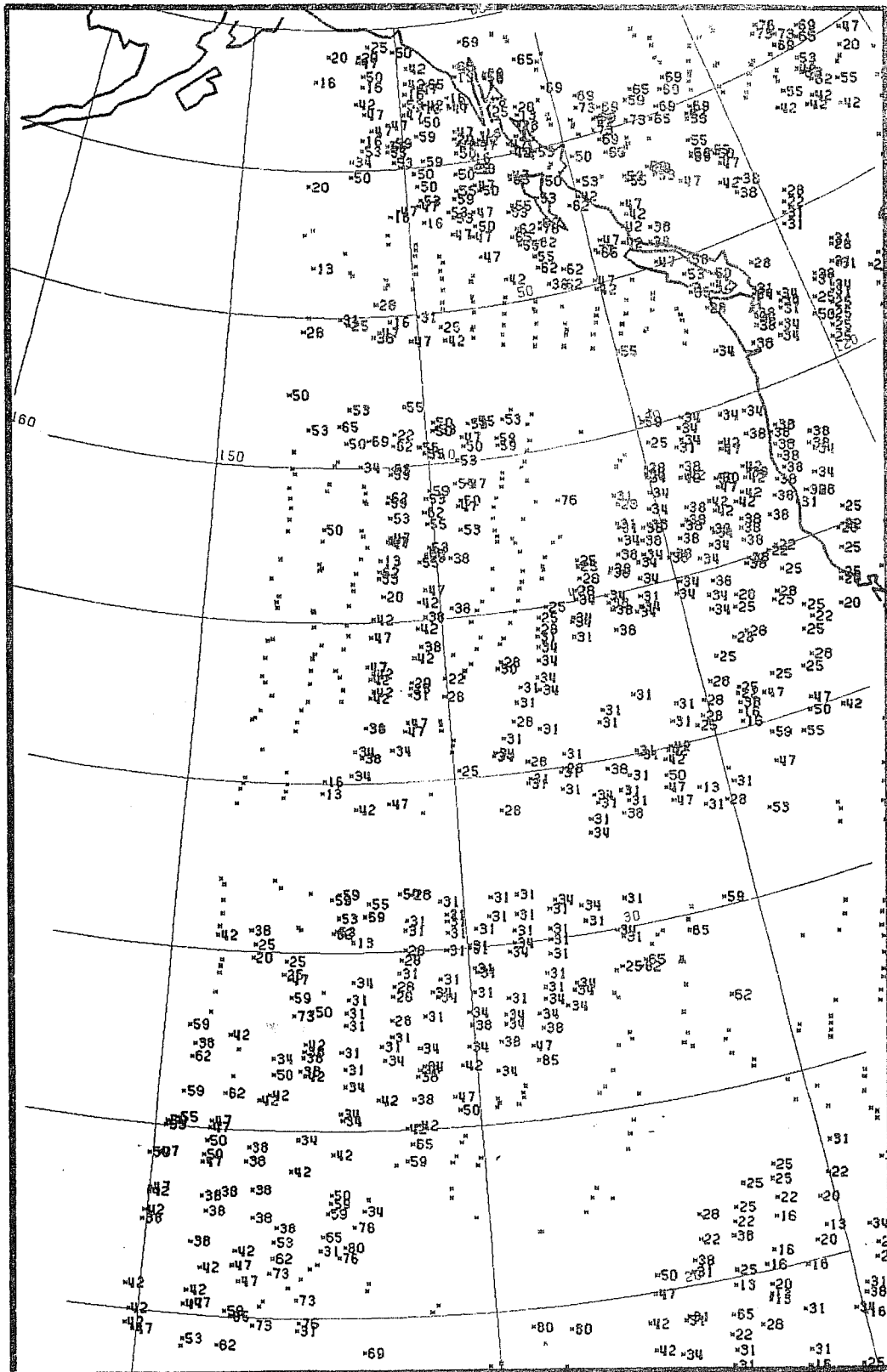


Figure 7b Same as Fig. 7a for the mean cloud top pressure (in 10 hPa).

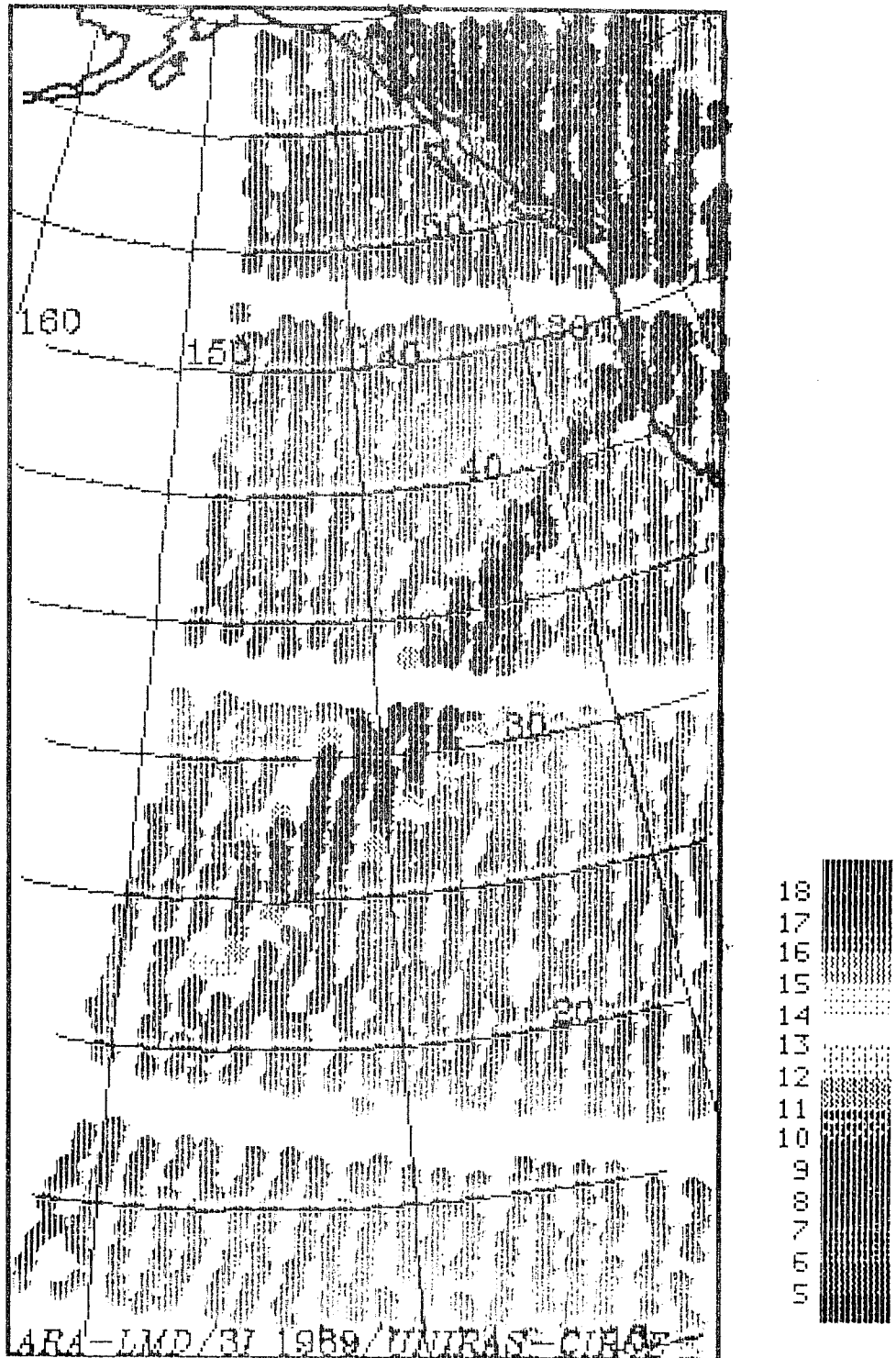


Figure 8 Map of the differences $MSU_2 - MSU_1$ for the same orbit as Fig. 7.

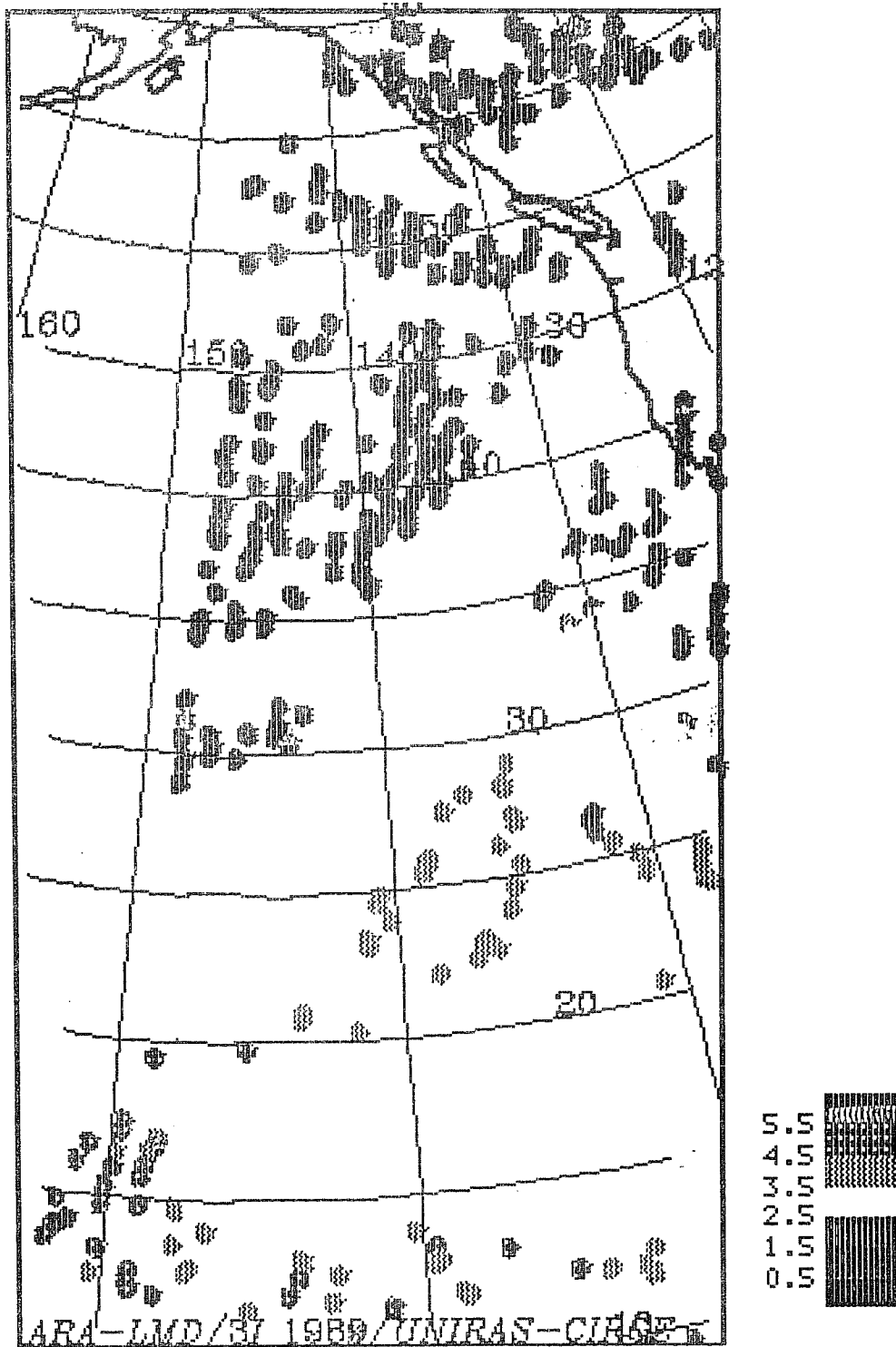


Figure 9 Total water vapor content retrieved by 3I. NOAA-9 pass 11018 (1st February 1987) (in precipitable cm).

Fig. 9 displays total water vapor contents as retrieved by 3I and shows high values ahead the front and much lower values after the front.

The front associated with this rain band is shown on Fig. 10 where the area for which the MSU difference is smaller or equal to 16°C has been superimposed.

6. CONCLUSIONS AND PERSPECTIVES

A recent extensive series of experiments conducted in ECMWF for measuring the impact of satellite retrieved products on middle range weather forecasting has brought into evidence positive as well as negative aspects of this data source. Concerning the 3I (Improved Initialization Inversion) scheme developed at LMD, positive aspects are related to the slightly better quality of the products on the average and, in particular, for the lowest layer 1000-850 hPa, their little random noise and better vertical gradients, their greater coherence in the horizontal, etc... Negative aspects were related to the appearance of too large biases over certain areas (Europe and North-East Canada, for example, the former however characterized by a strong anomalous circulation in the stratosphere with the stratospheric cold polar vortex being shifted from its "normal" location to Central Europe) and to too large differences in the overall tropospheric stability index when compared to the model first guess.

The modifications introduced in the 3I scheme to at least partly answer these questions are of three types :

- improvement of the procedure used to compute the temperature variance/covariance matrix involved in the estimation of the final solution ;
- refinement of the cloud clearing method ;
- introduction of a rain detection test rejecting microwave contaminated data and of a new cloud detection test for low clouds over sea ice.

Application of the modified code to several pathological NOAA-9 and NOAA-10 passes has shown very significant improvements over the former version. New results have been shown and compared to the "old" ones.

ECMWF experiments with 3I also suffered from an imperfect validation of the forward radiative transfer model and from the fact that the SSU

(Stratospheric Sounding Unit) data are not presently considered in the 3I processing.

New developments are presently being prepared in three directions :

- improvement of the validation by collecting radiosonde/satellite matched data of high quality with no angular or other pre-imposed corrections and involving a better air mass classification (work in progress at ECMWF ; G. Kelly, private communication) ;
- extension of the present TIGR data base from \approx 1200 situations to about 1600 situations in order to fill a few well identified "holes" ;
- refinement of the computation of the vertical and horizontal error correlation matrices for a better assimilation of satellite products in numerical prediction models.

These developments should certainly lead to new improvements in the quality of the retrievals.

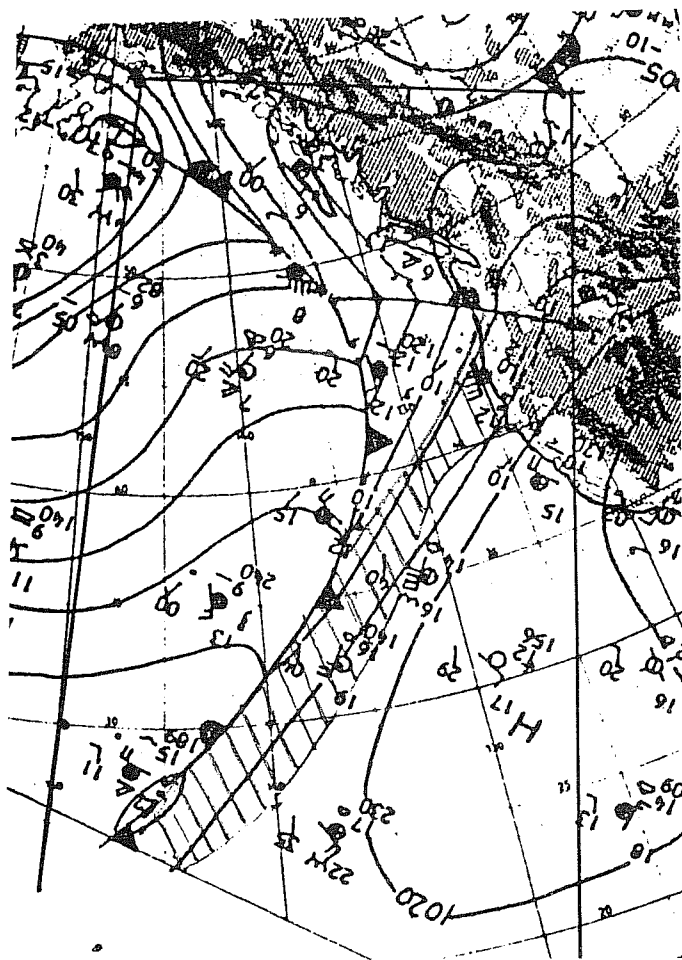


Fig. 10

Surface map for
1 February 1987
at \approx 12.00 UT
(from European
Meteorological
Bulletin).

REFERENCES

Andersson, E., A. Hollingsworth, G. Kelly, P. Lönnberg, J. Pailleux and Z. Zhang, 1989: Observing system experiments on NEDSIS statistical retrievals of TOVS satellite data using the 1988 ECMWF data assimilation system. In this volume.

Chedin, A., 1988: The 3I retrieval method. Recent local and global applications. Proceedings of the ECMWF Seminar on Data Assimilation and the Use of Satellite Data. Reading, 5-9 September 1988. To be published.

Chedin, A., N.A. Scott, C. Wahiche and P. Moulinier, 1985: The Improved Initialization Inversion method: a high resolution physical method for temperature retrievals from satellites of the TIROS-N series. *J. Clim. Appl. Meteor.*, **24**, 128-143.

Claude, C., A. Chedin, N.A. Scott and J.C. Gascard, 1989: Retrieval of mesoscale meteorological parameters for polar latitudes (MIZES and ARCTMEIZ campaigns). *Annales Geophysicae*, **7**, 205-212.

Flobert, J.C., E. Andersson, A. Chedin, G. Kelly, J. Pailleux and N.A. Scott, 1989: Data assimilation and forecast experiments at ECMWF using the 3I inversion scheme for satellite soundings. In this volume.

Phillips, N., 1980; Two examples of satellite temperature retrievals in the North Pacific. *Bull. Amer. Meteor. Soc.*, **61**, 712-717.

Acknowledgements

Authors are greatly indebted to T. Hollingsworth, J. Pailleux, G. Kelly and ECMWF staff members for very fruitful discussions and for their constant support.